

# Mapping of Highest Occupied Molecular Orbitals of Duplex DNA by Cobalt-Mediated Guanine Oxidation

Isao Saito,\* Takashi Nakamura, and Kazuhiko Nakatani

Contribution from the Department of Synthetic Chemistry and Biological Chemistry, Faculty of Engineering, Kyoto University, Kyoto 606-8501, Japan, and CREST, Japan Science and Technology Corporation

Received November 2, 1999

**Abstract:** We have examined the oxidation of oligodeoxynucleotides (ODN) containing various guanine (G)-containing sequences with Co(II) ion and benzoyl peroxide (BPO). Sequence-dependent G-cleavage has been observed for double-stranded ODN as revealed by PAGE analysis of the reaction mixture after hot piperidine treatment, whereas non-selective equal G cleavage was observed for single-stranded ODN. The relative rates of sequence-dependent G oxidation were determined by densitometric assay of the DNA cleavage bands. We then performed ab initio calculations of HOMOs of the G-containing sequences with B-form geometry at the HF/6-31G\* level. Experimentally observed relative rates of G oxidation matched well with the calculated HOMOs of the G-containing sequences. Thus, the DNA cleavage data obtained from the oxidation of duplex ODNs with Co(II) ion in the presence of BPO correlated nicely with calculated HOMOs, implying that the Co(II) ion is coordinated more strongly to the G having a larger HOMO. These results suggest that the coordination of Co(II) ion to the N<sub>7</sub> of guanine base in a duplex DNA is a HOMO-controlled process, in accordance with the previous NMR studies on the sequence-dependent binding of Co(II) ion to the N<sub>7</sub> of guanine base of duplex ODN. After performing ab initio calculations of a number of G-containing sequences, we found important general trends that represent the distribution of HOMOs of G bases in B-form DNA. The results of HOMO mapping described here are extremely important for predicting: (i) which G-sites are more susceptible to electrophilic attack in chemical and biological reactions, such as DNA alkylation by antitumor drugs or mutagens, and (ii) which G-sites are more prone to HOMO–LUMO interactions with DNA-binding drugs and proteins. These results provide a new tool for probing the heterogeneity of DNA sequences.

## Introduction

The highest occupied molecular orbital (HOMO) of organic molecules plays a crucial role in chemical reactions by interacting with the lowest unoccupied molecular orbital (LUMO) of reactant molecules.<sup>1</sup> Despite enormous contribution of HOMOs of small molecules in organic chemistry,<sup>2</sup> the HOMOs of naturally occurring macromolecules such as DNA and proteins have not been well recognized, because the calculation of the HOMOs of large molecules such as duplex DNA is extremely difficult, and as a consequence, experimental mapping of the HOMO of duplex DNA has not been undertaken. Consequently, there has been a lack of appreciation for the role HOMO–LUMO interactions play in DNA–drug and DNA–protein interactions, although HOMO–LUMO interactions between monomer guanine base and alkylating agents<sup>3</sup> or intercalators<sup>4</sup> have been investigated.

Theoretical calculations of DNA bases have been extensive for ionization potentials of monomeric nucleobases, for stability

of nucleobase-pair in neutral and radical cation states, and for stacking intereractions between nucleobases.<sup>5,6</sup> However, only a few ab initio calculations on stacked nucleobases have been reported.<sup>5d,e,6b</sup> Several years ago, we demonstrated experimentally and by theoretical calculations that the HOMO of a stacked 5'-GG-3' sequence is especially high in energy and concentrated on the 5'-G.<sup>6</sup> As a consequence, one-electron oxidation and electrophilic attacks are favored at this site.<sup>6,7</sup> We recently reported a precise mapping of G-rich hot spots in DNA one-electron oxidation such as stacked GG doublets and GGG triplets by ab initio MO calculations.<sup>8</sup> We also calculated the radical cation and neutral radical stages of various stacked GGG triplets to examine the detail analyses of the selectivity of GGG triplets toward photoinduced one-electron oxidation.<sup>9</sup>

In the current study, we performed ab initio calculations of HOMOs of a wide variety of G-containing sequences with

\* To whom correspondence should be addressed. Telephone: 81-75-753-5656. Fax: +81-75-753-5676. E-mail: saito@sbchem.kyoto-u.ac.jp.

(1) Fukui, K. *Accounts Chem. Res.* **1971**, *4*, 57.

(2) See, for example: Fleming, I. Ed. In *Frontier Orbitals and Organic Reactions*; Wiley-Interscience: New York, 1976.

(3) (a) Broch, H.; Hamza, A.; Vasilescu, D. *J. Biomol. Struct. Dyn.* **1996**, *13*, 903. (b) Hamza, A.; Broch, H.; Vasilescu, D. *J. Biomol. Struct. Dyn.* **1996**, *13*, 915. (c) Patterson, S. E.; Coxon, J. M.; Strekowski, L. *Bioorg. Med. Chem.* **1997**, *5*, 277.

(4) Nakatani, K.; Okamoto, A.; Matsuno, T.; Saito, I. *J. Am. Chem. Soc.* **1998**, *120*, 11219.

(5) (a) Hutter, M.; Clark, T. *J. Am. Chem. Soc.* **1996**, *118*, 7574. (b) Colson, A.-O.; Besler, B.; Close, D. M.; Sevelia, M. D. *J. Phys. Chem.* **1992**, *96*, 661. (c) Alhambra, C.; Luque, F. J.; Gago, F.; Orozco, M. *J. Phys. Chem.* **1997**, *101*, 3846. (d) Sponer, J.; Leszczynski, J.; Hobza, P. *J. Phys. Chem.* **1996**, *100*, 5590. (e) Prat, F.; Houk, K. N.; Foote, C. S. *J. Am. Chem. Soc.* **1998**, *120*, 845.

(6) (a) Saito, I.; Takayama, M.; Sugiyama, H.; Nakatani, K.; Tsuchida, I.; Yamamoto, M. *J. Am. Chem. Soc.* **1995**, *117*, 6406. (b) Sugiyama, H.; Saito, I. *J. Am. Chem. Soc.* **1996**, *118*, 7063.

(7) For a review, see: Burrows, C. J.; Muller, J. G. *Chem. Rev.* **1998**, *98*, 1109.

(8) Saito, I.; Nakamura, T.; Nakatani, K.; Yoshioka, Y.; Yamaguchi, K.; Sugiyama, H. *J. Am. Chem. Soc.* **1998**, *120*, 12686.

(9) Yoshioka, Y.; Kitagawa, Y.; Takano, Y.; Yamaguchi, K.; Nakamura, T.; Saito, I. *J. Am. Chem. Soc.* **1999**, *121*, 8712.

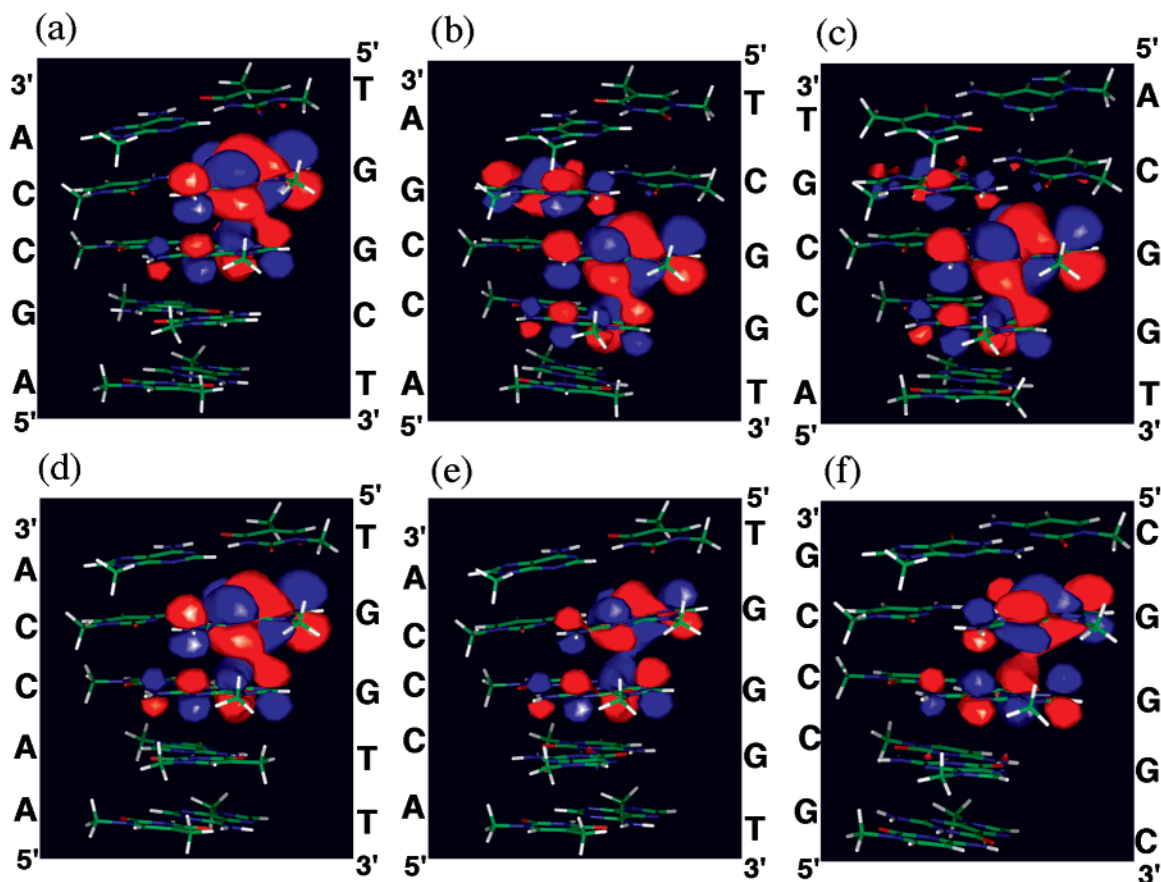


**Figure 1.** Orbital contour plot of the HOMOs of six B-form DNA 5-mers obtained by ab initio calculations using GAUSSIAN 94<sup>10</sup> at the HF/6-31G\* level. The sequences are shown on both sides. The sugar backbones were replaced by methyl groups.

B-form geometry and compared these data with the experimental results obtained from the oxidation of the same G-containing sequences with cobalt (II) ion and benzoyl peroxide (BPO). For a wide range of DNA sequences, the experimentally obtained data matched well with the calculated HOMOs, and several interesting general trends were observed for the HOMO distribution in B-form DNA.

## Results and Discussion

**HOMOs of G-Containing DNA Sequences obtained by Ab Initio Calculations.** We performed ab initio calculations of HOMOs for a wide variety of G-containing sequences with B-form geometry using GAUSSIAN 94<sup>10</sup> at the HF/6-31G\* level. Double strands of B-form 5-mers containing a variety of G sequences were built using the Insight II program with standard B-form parameters. For the quantum mechanical studies, all of the sugar backbones of the duplex 5-mers were removed from the coordinate file (while keeping the positions of all of the atoms fixed) and replaced by methyl groups.<sup>5c,6b,8,9</sup> The orbital contour plots of the calculated HOMOs of typical duplex 5-mers are shown in Figure 1, and the distributions of HOMOs are summarized in Figure 2. As seen in Figure 1a, the HOMO of the duplex 5'-TGGCT-3'/3'-ACCGA-5' sequence was

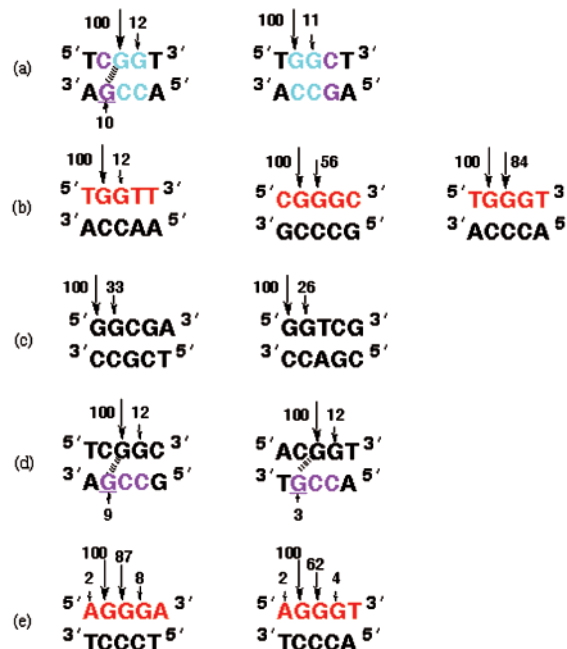


**Figure 2.** Distribution of HOMOs in duplex 5-mers obtained by ab initio HF/6-31G\* single-point calculations. The arrows indicate the distribution of the HOMOs normalized the largest HOMO as 100. The broken line emphasizes the stacking of the single G of 5'-CCG-3' sequence with the 5'-G of the GG doublet on the opposite strand.

largely localized on the 5'-G of the GG doublet, with no HOMO at the single G (underlined). In contrast, in another duplex (5'-TCGGT-3'/3'-AGCCA-5'; Figure 1b), the HOMO distribution at the single G (underlined) was considerably large. The only

(10) Frisch, M. J.; Trucks, G. W.; Schlegel, H. B.; Gill, P. M. W.; Johnson, B. G.; Robb, M. A.; Cheeseman, J. R.; Keith, T.; Petersson, G. A.; Montgomery, J. A.; Raghavachari, K.; Al-Laham, M. A.; Zakrzewski, V. G.; Ortiz, J. V.; Foresman, J. B.; Cioslowski, J.; Stefanov, B. B.; Nanayakkara, A.; Challacombe, M.; Peng, C. Y.; Ayala, P. Y.; Chen, W.; Wong, M. W.; Andres, J. L.; Replogle, E. S.; Gomperts, R.; Martin, R. L.; Fox, D. J.; Binkley, J. S.; Defrees, D. J.; Baker, J.; Stewart, J. P.; Head-Gordon, M.; Gonzalez, C.; Pople, J. A. *Gaussian 94*, revision E.2; Gaussian, Inc.: Pittsburgh, PA, 1995.

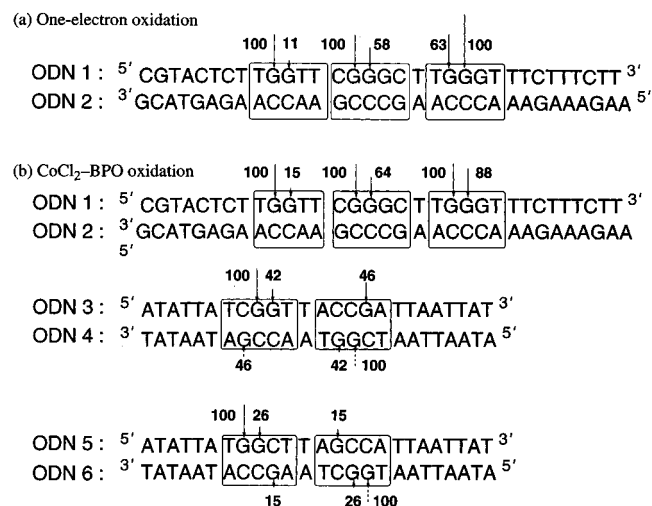


**Figure 3.** Intensities of the DNA cleavage bands. The intensities were normalized by assigning a value of 100 to the largest cleavage band in each segment (as indicated by the block). The arrows indicate the cleavage sites. (a) Photooxidation of duplex DNA in the presence of riboflavin. (b) Oxidation of duplex DNA with CoCl<sub>2</sub>-BPO.

difference between these duplexes was that the GG doublet was flanked on either the 5' side or the 3' side by a G-C base pair as illustrated in Figure 2a. Thus, the ab initio calculations clearly indicated that the HOMO localization on G base is highly sequence-dependent.

**General Trends for the HOMO Distributions in B-Form DNA.** After performing ab initio calculations of a number of G-containing sequences, we found important general trends that represent the distribution of HOMOs of G bases in B-form DNA. First, the HOMOs of stacked GG doublets are localized overwhelmingly on the 5'-G, regardless of the 3'- and 5'-flanking sequences (A, C, or T). Second, in stacked GGG triplets (Figure 2b,e), the HOMO distribution is always greater for the 5'-G than for the middle G with almost no HOMO at the 3'-G, regardless of the 3'- and 5'-flanking sequences (A, C, or T). Another important feature is that the single Gs of 5'-CCG-3' sequences have exceptionally large HOMOs compared with those of the single Gs of other sequences (Figure 1b). It should be noted that in 5'-CCG-3' sequences, the single G (underlined) is significantly overlapped with the 5' side G of the GG doublet on the opposite strand (Figure 2a,d). A similar feature has also been observed on the extraordinary high HOMO energies of 5'-CGG-3'/3'-GCC-5' sequence compared with those of other GG doublets due to the large overlap of the single G (underlined) with the 5'G of the GG doublet on the opposite strand.<sup>8,9</sup> The calculated HOMOs of the G-containing sequences shown in Figure 2 can predict the relative susceptibility of each G toward electrophilic attack and HOMO-LUMO interactions with the LUMO of DNA-binding molecules.

**An Attempt for Experimental HOMO Mapping.** We have then attempted an experimental mapping of the HOMO of duplex DNA. As a mapping probe, we used an oligodeoxynucleotide (ODN) containing 5'-TGGTT-3', 5'-CGGCG-3' and 5'-TGGGT-3' sequences (ODN 1; Figure 3). In one-electron oxidation such as riboflavin-sensitized photooxidation, the 5'-Gs of 5'-TGGT-3' and 5'-CGGCG-3' sequences have been known to be selectively oxidized,<sup>6a,9,11</sup> while 5'-TG<sub>1</sub>G<sub>2</sub>G<sub>3</sub>T-3'

was preferentially oxidized at G<sub>2</sub> as shown in Figure 3a<sup>6a,9,12</sup>. These results, particularly those of the 5'-TGGGT-3' sequence are not in agreement with the calculated HOMOs (cf. Figure 2b vs Figure 3a). In contrast, recent <sup>1</sup>H NMR studies of the coordination of the Co(II) ion to the N<sub>7</sub> of G in DNA oligomers, have shown that the binding selectivity of the Co(II) ion toward 5'-TG<sub>1</sub>G<sub>2</sub>G<sub>3</sub>T-3' sequence follows the order G<sub>1</sub> > G<sub>2</sub> >> G<sub>3</sub> while holding a high 5'-G selectivity for GG doublets.<sup>13</sup> These binding selectivities are quite compatible with the calculated HOMOs of Figure 2b. Crystallographic studies have indicated that the Co(II) ion binds exclusively to the N<sub>7</sub> of G by coordination.<sup>14</sup> We, therefore, assumed that the coordination of low concentrations of Co(II) ion, a soft Lewis acid, to the N<sub>7</sub> of electron-rich G is a HOMO-controlled process, and as a consequence, the sequence selectivity of the Co(II) ion binding obtained from the <sup>1</sup>H NMR studies would directly reflect the HOMO distribution in G-containing sequences.

**Comparison of Cobalt-Mediated G-Oxidation with Calculated HOMO.** Previously, Co(II) ion has been shown to mediate G oxidation in the presence of oxidants such as HSO<sub>5</sub><sup>-</sup> to produce piperidine labile sites.<sup>15</sup> It has also been reported that sequence-selective G cleavage was observed in the oxidation of DNA with BPO in the presence of CuCl.<sup>16</sup> With these in mind, we performed DNA cleavage experiments in the presence of low concentrations of Co(II) ion, using benzoyl peroxide (BPO) as an oxidant. Incubation of the double-stranded <sup>32</sup>P-5'-end-labeled ODN 1/2 with Co(II) ion (such as CoCl<sub>2</sub> or Co(OAc)<sub>2</sub>) and BPO at 37 °C for 5 min, followed by treatment with hot piperidine, resulted in a highly selective G cleavage (Figure 4, lanes 1 and 2). The degree of cleavage was then determined using a densitometric assay. For direct comparison with the calculated HOMO data, the cleavage data was normalized by assigning a value of 100 to the largest cleavage band in each segment (as indicated by the block shown in Figure 3). The DNA cleavage data of duplex ODN 1/2 was in complete agreement with the calculated HOMOs (cf. Figure 2b vs Figure 3b). In contrast, using identical conditions to the ODN 1/2 cleavage reaction, the single-stranded ODN 1 without ODN 2 showed non-selective G cleavage (lanes 3 and 4).

It has been reported that a high concentration of Co(II) ion induced a conformational change of B-form DNA containing G-rich sequences.<sup>17</sup> To confirm whether Co(II) ion induces a conformational change of these G-containing duplex ODN under the reaction conditions, we measured the CD spectrum of a duplex 5'-CATTTCGGGCTTG-3'/5'-CAAGCCCCGAAATG-3'. However, no conformational change has been observed upon addition of CoCl<sub>2</sub> up to 200 μM (20 equiv to ODN) under the DNA cleavage reaction conditions as shown in Figure 5.

(12) (a) Saito, I.; Takayama, M.; Sugiyama, H.; Nakamura, T. In *DNA and RNA Cleavers and Chemotherapy of Cancer and Viral Diseases*; Meunier, B., Ed.; NATO ASI Series; Kluwer Academic Publishers: Dordrecht, The Netherlands, 1996; pp 163. (b) Ito, K.; Inoue, S.; Yamamoto, K.; Kawanishi, S. *J. Biol. Chem.* **1993**, *268*, 13221. (c) Ito, K.; Kawanishi, S. *Biochemistry* **1997**, *36*, 1774. (d) Spassky, A.; Angelov, D. *Biochemistry* **1997**, *36*, 6571. (e) Meggers, E.; Michel-Beyerle, M. E.; Giese, B. *J. Am. Chem. Soc.* **1998**, *120*, 12950. (f) Hall, D. B.; Kelley, S. O.; Barton, J. K. *Biochemistry* **1998**, *37*, 15933.

(13) Moldrheim, E.; Andersen, B.; Froystein, N. A.; Sletten, E. *Inorg. Chim. Acta* **1998**, *273*, 41.

(14) Gao, Y.-G.; Sriam, M.; Wang, A. H.-J. *Nucleic Acids Res.* **1993**, *21*, 4093.

(15) Muller, J. G.; Zheng, P.; Rokita, S. E.; Burrows, C. J. *J. Am. Chem. Soc.* **1996**, *118*, 2320.

(16) (a) Akman, S. A.; Kensler, T. W.; Doroshow, J. H.; Dizdaroglu, M. *Carcinogenesis* **1993**, *14*, 1971. (b) Kawanishi, S.; Oikawa, S.; Murata, M.; Tsukitome, H.; Saito, I. *Biochemistry* **1999**, *38*, 16733.

(17) Xu, Q.; Shoemaker, R. K.; Braunlin, W. H. *Biophys. J.* **1993**, *65*, 1039.

(11) (a) Hall, D. B.; Holmin, R. E.; Barton, J. K. *Nature* **1996**, *382*, 731. (b) Holmin, R. E.; Dandliker, P. J.; Barton, J. K. *Angew. Chem., Int. Ed. Engl.* **1997**, *36*, 2714.



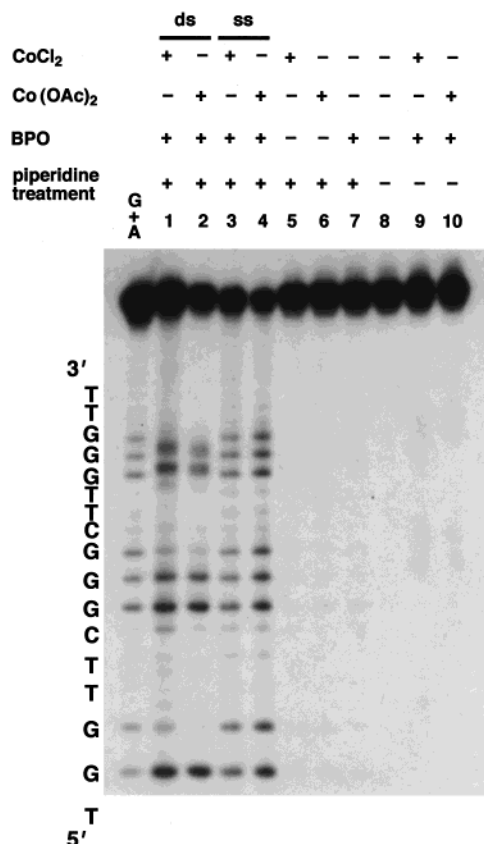


**Figure 4.** Autoradiogram of the denaturing gel of the <sup>32</sup>P-5'-end-labeled duplex ODN 1/2 after incubation with BPO in the presence of cobalt ion. <sup>32</sup>P-5'-end-labeled ODN 1 was hybridized to the complementary ODN 2, and the duplex was incubated with BPO and cobalt ion as described in the Experimental Section.

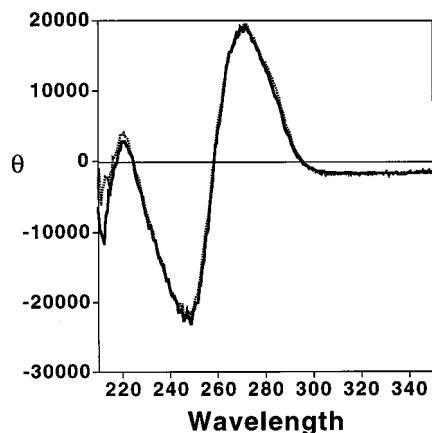


**Figure 5.** CD spectra of 5'-CATTTCGGGCTTG-3'/5'-CAAGC-CCGAAATG-3' (10  $\mu$ M, strand concentration) in 10 mM sodium cacodylate buffer (pH 7.0) and NaCl 100 mM at 37  $^{\circ}$ C. The solid line is in the presence of Co(II) (200  $\mu$ M), and the dotted line is in the absence of Co(II).

Next, we examined the HOMO mapping of other duplexes ODN 3/4 and ODN 5/6 by comparing the reactivity of the 5'-CCG-3' sequence possessing a larger HOMO with that of the 5'-GCC-3' sequence using a GG doublet as an internal standard. As shown in Figure 6 (lanes 1 and 8), the 5'-CCG-3' sequence had a much higher reactivity than the 5'-GCC-3' sequence, as predicted from the calculated HOMOs (Figure 2a). The DNA cleavage data shown in Figure 6 are again in good agreement with the calculated HOMOs.

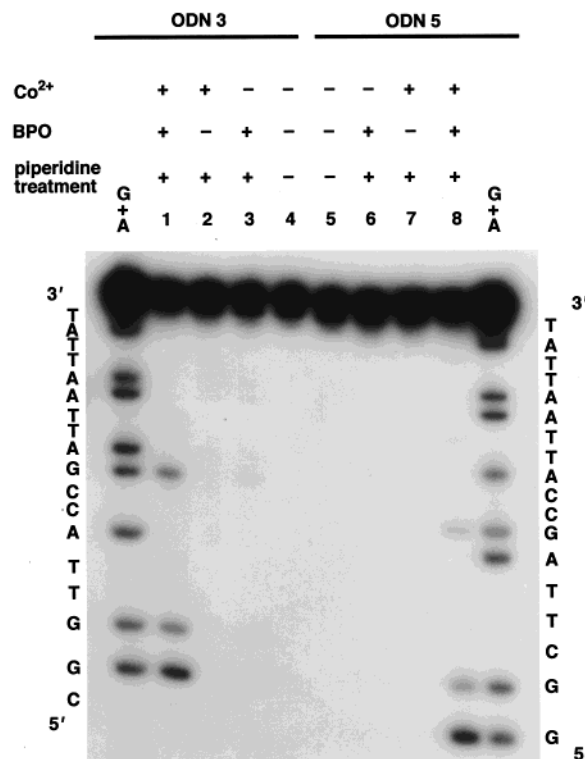


**Figure 6.** Autoradiogram of the denaturing gel of the <sup>32</sup>P-5'-end-labeled duplex ODNs after incubation with BPO in the presence of cobalt ion. <sup>32</sup>P-5'-end-labeled ODN 3 and <sup>32</sup>P-5'-end-labeled ODN 5 were hybridized to ODN 4 and ODN 6, respectively. The <sup>32</sup>P-5'-end-labeled duplexes were incubated with BPO (10  $\mu$ M, final concn) in the presence of cobalt ion (3  $\mu$ M, final concn) as described in the Experimental Section.

While the DNA cleavage data experimentally obtained are fully consistent with the hypothesis that Co(II) ion is coordinated more strongly to the guanine N<sub>7</sub> having a larger HOMO, there seems to be an alternative explanation. Positively charged cobalt ion would bind to the most negative G sites in duplex DNA via an electrostatic interaction. We, therefore, examined the ab initio calculations of molecular electrostatic potentials<sup>18</sup> (MEPs) for two duplexes, 5'-TCGG-3'/5'-CCGA-3' and 5'-TGGC-3'/5'-GCCA-3'. The MEPs were calculated at the HF/3-21G level and compared with the calculated HOMOs of the same duplexes. In the electrostatic potential map of Figure 7b, pink and blue indicate negative electrostatic potential. In both duplexes, the difference of the negative electrostatic potentials between the 5'-G and the 3'-G of GG doublet was not so large as that observed for HOMO, inconsistent with the experimental results (cf. Figure 7b vs 7a). We also performed ab initio calculations of the total atomic charges of all the guanine N<sub>7</sub>'s for the two duplexes at the HF/6-31G\* level. As shown in Figure 7c, the total atomic charge of N<sub>7</sub> (-0.55405) for the single G (underlined) of duplex 5'-TCGG-3'/5'-CCGA-3' was much larger than that of the 5'-G (-0.55047) of GG doublet, quite inconsistent with the experimental results. Thus, the calculated total atomic charges and Pullman's MEPs cannot fully explain the results of ODN 3/4 and ODN 5/6 shown in Figure 3b, although sequence selective guanine N<sub>7</sub> alkylation of contiguous Gs by positively charged DNA alkylating agents has been explained reasonably by MEPs.<sup>19</sup> All of the experimental results

(18) Pullman, A.; Pullman, B. *Q. Rev. Biophys.* **1981**, *14*, 289.

(19) (a) Kohn, K. W.; Hartley, J. A.; Mattes, W. B. *Nucleic Acids Res.* **1987**, *15*, 10531. (b) Warpehoski, M. A.; Hurley, L. H. *Chem. Res. Toxicol.* **1988**, *1*, 315.

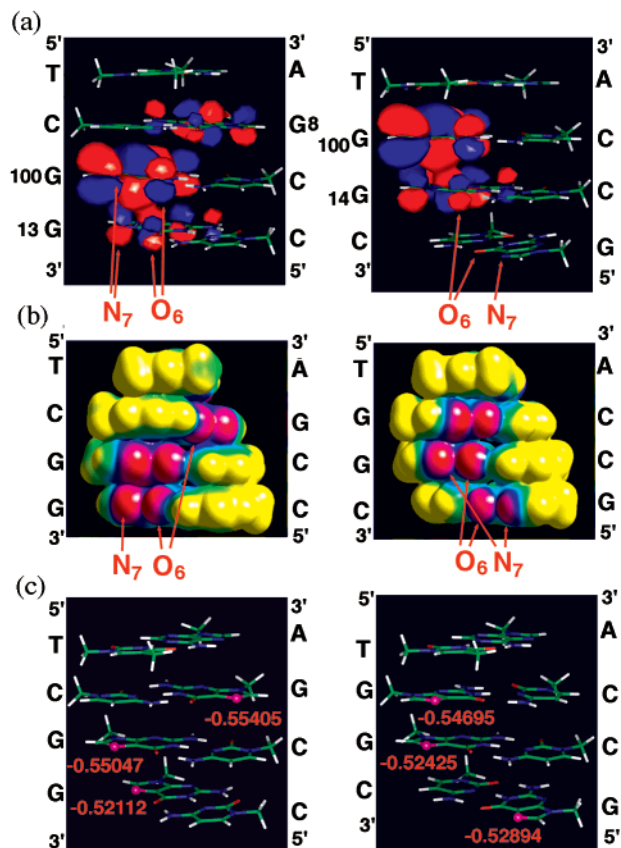


**Figure 7.** Comparison of orbital contour plot of HOMOs (a), molecular electrostatic potential (MEP) maps (b), and total atomic charges of guanine N<sub>7</sub> (c) for two duplexes, 5'-TCGG-3'/5'-CCGA-3' and 5'-TGGC-3'/5'-GCCA-3'. (a) Ab initio calculations at the HF/3-21G level. The sequences are shown on both sides. The sugar backbones were replaced by methyl groups. The values on both sides indicate the distribution of the HOMOs normalized the largest HOMO as 100. (b) In the electrostatic potential map, pink and blue indicate negative electrostatic potentials, and yellow and green represent positive electrostatic potentials. (c) Total atomic charges of guanine N<sub>7</sub> (pink sphere). The sequences are shown on both sides. The sugar backbones were replaced by methyl groups. The values (red) were calculated at the HF/6-31G\* level.

are best explained by the calculated HOMOs, that is, the experimental data obtained by the CoCl<sub>2</sub>-BPO reaction are consistent with the assumption that cobalt ion binds most strongly to the G having a largest HOMO, although there is no direct proof to support that the G oxidation is a HOMO-controlled reaction.

To get insight into the mechanism of the G oxidation, we analyzed the reaction mixture obtained from the incubation (37 °C, 2.5 h) of self-complementary ODN, 5'-ATGGGTACCCAT-3' with CoCl<sub>2</sub> and BPO under the same conditions as those for DNA cleavage experiments followed by enzymatic digestion. Due to the complexity of the reaction mixture together with low conversion of the ODN, attempts to isolate the oxidation products were unsuccessful. However, by the HPLC analysis of the mixture, the formation of a small amount of 7,8-dihydro-8-oxo-2'-deoxyguanosine (8-oxo-dG) was confirmed by comparison of the HPLC retention time and the UV spectrum obtained by photodiodearray assay with those of authentic sample. It should be noted that 8-oxo-dG was also produced in the oxidation of DNA with CuCl and BPO.<sup>16b</sup>

## Conclusions

We were able to demonstrate for the first time the experimental HOMO mapping of duplex DNA using cobalt ions and benzoyl peroxide, in combination with ab initio calculations of a wide variety of G-containing DNA sequences. The simple HOMO mapping method described in this study may allow its application to other nucleic acids, such as different forms of DNA, DNA-RNA hybrids, and RNA. The HOMOs shown in Figure 2 provide a simple way of predicting the sequence-dependent reactivity of G bases in duplex DNA and their susceptibility to HOMO-LUMO or charge-transfer interactions with electron-accepting functional groups of DNA-binding drugs and proteins. While noncovalent intermolecular forces such as electrostatic interactions, stacking interactions, hydrogen bonding, and hydrophobic effects are well-known for DNA-ligand and DNA-protein interactions,<sup>20</sup> the interaction of DNA HOMOs with the LUMOs of DNA-binding molecules could also be another important binding force. The present HOMO mapping method can visualize the susceptibility of G-containing sequences to HOMO-LUMO interactions with DNA-binding molecules including transition metal ions, thus providing a new tool for probing the heterogeneity of DNA sequences. These results have led to a new view of the chemical and physicochemical properties of DNA and the sequence-dependent reactions of G bases in DNA. The consequence of HOMO-LUMO interactions in metal-DNA, drug-DNA, or protein-DNA interactions is clearly an important area to be investigated in future studies.

## Experimental Section

**General.** Cobalt chloride (CoCl<sub>2</sub>) was purchased from Nacalai Tesque Co., Ltd. Benzoyl peroxide (BPO) was purchased from Wako Pure Chemical Industries, Ltd. Calf thymus DNA (1 g) was purchased from Pharmacia Biotech. The oligodeoxynucleotides were purchased from Amersham Pharmacia Biotech. T4 kinase was purchased from NIPPON GENE (10 units/μL) and γ-[<sup>32</sup>P]-ATP (10 mCi/ml) was from Amersham. All aqueous solutions utilized purified water (MILLIPORE, Mili-Q sp UF). A GIBCO BRL model S2 sequencing gel electrophoresis apparatus was used for polyacrylamide gel electrophoresis (PAGE).

**Theoretical Calculations.** Ab initio calculations were performed at the HF/3-21G level for molecular electrostatic potentials (MEPs) and at the HF/6-31G\* level for other calculations utilizing the GAUSSIAN 94 program package.<sup>10</sup> Geometries of the duplex consisting of stacked methylated nucleobases at N<sub>1</sub> (pyrimidine base) and N<sub>9</sub> (purine base) were constructed as follows.<sup>6b,8,9</sup> The corresponding duplex 4-mers or 5-mers were built using the insightII program (Version 97.0) with standard B-form helical parameters (pitch, 3.38 Å; twist, 36°; tilt, 1°) which have been optimized by X-ray crystallographic analysis of relevant monomers and X-ray diffraction data of polymers.<sup>21</sup> All of the sugar backbones of the duplex were removed except for the deoxyribose C1' carbon and C1' H and two H atoms were then attached to the C1' methine to complete stacked N-methylated nucleobases, keeping the position of all atoms fixed. HOMOs of the calculated 5-mers were displayed graphically using Gaussian/F. MEPs were displayed graphically using Cerius<sup>2</sup> (Version 3.8).

**DNA Cleavage Experiments using Cobalt ion and BPO.** The <sup>32</sup>P-end-labeled ODNs were hybridized to their complementary ODNs (2.5 μM, strand concentration) in 10 mM sodium cacodylate buffer (pH 7.0). Hybridization was achieved by heating the samples to 90 °C for 5 min and then slowly cooling the samples to room temperature. The <sup>32</sup>P-end-labeled duplex solutions were added to a 1.5 mL Eppendorf tube containing 35 μL of MilliQ water, 20 μL of 50 μM aqueous cobalt chloride or 50 μM cobalt acetate solution (15 μM, final concentration), and 5 μL of freshly prepared 1 mM BPO solution in acetonitrile (50 μM, final conc). After incubation at 37 °C for 5 min, the solutions

(20) For example, Neidle, S. In *DNA Structure and Recognition*; Rickwood, D., Ed.; Oxford University Press: New York, 1994; Vol. 71.

(21) (a) Arnott, S.; Hukins, D. W. L. *Biochem. Biophys. Res. Commun.* **1972**, *47*, 1504. (b) Arnott, S.; Selsing, E. *J. Mol. Biol.* **1974**, *88*, 509.

were diluted with 10  $\mu\text{L}$  of calf thymus DNA (50  $\mu\text{M}$ , base pair conc) and 10  $\mu\text{L}$  of 3 M sodium acetate buffer (pH 5.2). After precipitation with cold ethanol (800  $\mu\text{L}$ ) for 20 min at  $-80\text{ }^\circ\text{C}$  followed by centrifugation (15 min at  $0\text{ }^\circ\text{C}$ ,  $1.5 \times 10^4$  rpm), the resulting DNA pellets were washed with cold 80% ethanol and dried under vacuum using a Speedvac. After the DNA pellets were treated with 1 M piperidine for 20 min at  $90\text{ }^\circ\text{C}$ , the solution was evaporated under vacuum, and the piperidine was coevaporated with water twice. The radioactivity of the samples was then assayed using an Aloka 1000 liquid scintillation counter, and the dried samples were dissolved in 80% formamide loading buffer (to reach to a radiation density of 2000–3000 cpm/ $\mu\text{L}$ ) and electrophoresed through a denaturing 12% polyacrylamide/7 M urea gel (1900 V, 1.5 h). The gels were exposed to X-ray film with an intensifying screen at  $-70\text{ }^\circ\text{C}$ . The degree of DNA cleavage was assayed using a BIORAD model GS-700 Imaging densitometer and BIORAD Molecular Analyst software (Version 2.1).

**CD Measurement.** CD spectra were measured on a JASCO J-720 spectropolarimeter. The ODNs (10  $\mu\text{M}$ , strand concentration) were hybridized in 10 mM sodium cacodylate buffer at pH 7.0 containing NaCl (100 mM). Hybridization was achieved by heating the sample to  $90\text{ }^\circ\text{C}$  for 5 min and then slowly cooling the sample to room

temperature. Aqueous cobalt chloride (200  $\mu\text{M}$ , final concentration) was added before CD measurement. The sample solution was measured at  $37\text{ }^\circ\text{C}$ . CD data were transformed into molar ellipticity [ $\theta$ ] in the units of degree  $\text{cm}^2/\text{dm}$  of monomer subunits.

**Acknowledgment.** We are grateful to the Supercomputer Laboratory, Institute for Chemical Research, Kyoto University, for providing computation time. We thank Drs. Hiroshi Sugiyama, Tokyo Medical & Dental University, Yasunori Yoshioka and Kizashi Yamaguchi, Osaka University, and Takashi Morii, Kyoto University, for helpful discussions.

**Supporting Information Available:** Autoradiograms of cobalt-mediated DNA cleavage of other sequences, their calculated HOMOs and HPLC analysis of the reaction mixture obtained by cobalt-mediated oxidation of self-complementary oligonucleotide (PDF). This material is available free of charge via the Internet at <http://pubs.acs.org>.

JA993891N